

- ³W. T. Stacy, A. B. Voermans, and H. Logmans, *J. Appl. Phys.* **48**, 4634 (1977).
- ⁴S. Konishi, T. Kawamoto, and M. Wada, *IEEE Trans. Magn. MAG-10*, 642 (1974); S. Konishi, T. Miyama, and K. Ikeda, *Appl. Phys. Lett.* **27**, 258 (1975).
- ⁵A. H. Bobeck, I. Danylchuk, J. P. Remeika, L. G. Van Uitert, and E. M. Walters, *Proc. International Conference on Ferrites, Kyoto, 1970*, p. 361.
- ⁶C. H. Tsang and R. L. White, *AIP Conf. Proc.* **24**, 749 (1975); C. H. Tsang, R. L. White, and R. M. White, *AIP Conf. Proc.* **29**, 552 (1976).
- ⁷M. V. Chetkin, A. N. Shalygin, and A. de la Campa, *Fiz. Tverd. Tela* **19**, 3470 (1977) [*Sov. Phys. Solid State* **19**, 2029 (1977)].
- ⁸M. V. Chetkin and A. de la Campa, *Pis'ma Zh. Eksp. Teor. Fiz.* **27**, 168 (1978) [*JETP Lett.* **27**, 157 (1978)].
- ⁹F. H. De Leeuw and J. M. Robertson, *J. Appl. Phys.* **46**, 3182 (1975).
- ¹⁰M. V. Chetkin, Yu. S. Didosyan, A. I. Akhutkina, and A. Ya. Chervonenkis, *Pis'ma Zh. Eksp. Teor. Fiz.* **12**, 519 (1970) [*JETP Lett.* **12**, 363 (1970)].
- ¹¹A. S. Borovik-Romanov, *Problemy magnetizma (Problems of Magnetism)*, Nauka, 1972, p. 47.
- ¹²K. P. Belov and A. M. Kadomtseva, *Usp. Fiz. Nauk* **103**, 577 (1971) [*Sov. Phys. Usp.* **14**, 154 (1971)].
- ¹³F. B. Hagedorn, *AIP Conf. Proc.* **5**, 72 (1972).
- ¹⁴V. G. Bar'yakhtar, B. A. Ivanov, and A. L. Sukstanskiĭ, *Pis'ma Zh. Eksp. Teor. Fiz.* **27**, 226 (1978) [*JETP Lett.* **27**, 211 (1978)].
- ¹⁵A. S. Borovik-Romanov, V. G. Zhotikov, N. M. Kreĭnes, and A. A. Pankov, *Pis'ma Zh. Eksp. Teor. Fiz.* **23**, 705 (1976) [*JETP Lett.* **23**, 649 (1976)].
- ¹⁶J. R. Shane, *Phys. Rev. Lett.* **20**, 728 (1968).
- ¹⁷T. A. Kraftmakher, V. V. Meriakri, and A. Ya. Chervonenkis, *Zh. Eksp. Teor. Fiz.* **70**, 172 (1976) [*Sov. Phys. JETP* **43**, 90 (1976)].

Translated by W. F. Brown, Jr.

Crystal structure, and magnetic and magnetoelastic properties of UGa_2

A. V. Andreev, K. P. Belov, A. V. Deryagin, Z. A. Kazeĭ, R. Z. Levitin, A. Meňovský,¹⁾ Yu. F. Popov, and V. I. Silant'ev

*M. V. Lomonosov State University, Moscow
and A. M. Gor'kii Ural State University, Sverdlovsk
(Submitted 13 June 1978)
Zh. Eksp. Teor. Fiz.* **75**, 2351-2361 (December 1978)

An investigation was made of the temperature dependences of the crystal lattice parameters, saturation magnetization, paramagnetic susceptibility, coercive force, and magnetostriction of single crystals of the intermetallic compound UGa_2 . In the magnetically ordered state ($T_c = 125^\circ K$), the magnetic moment of uranium is $2.71 \mu_B$ and it is due to the partly delocalized $5f$ electrons. Below T_c , the compound UGa_2 experiences a strong orthorhombic distortion of the hexagonal lattice which is due to large magnetostrictive strains ($\lambda \sim 10^{-3}$). There is a considerable magnetocrystalline anisotropy in the ferromagnetic and paramagnetic states. The uniaxial magnetic anisotropy constant is $K_1 = -2 \times 10^7$ erg/g and the constant representing anisotropy in the basal plane is $K_3 = -0.6 \times 10^6$ erg/g.

PACS numbers: 75.30.Cr, 75.80.+q, 75.30.Gw, 61.80.+m

1. INTRODUCTION

The magnetic properties and crystal structures of uranium compounds are of considerable interest in the physics of magnetism and magnetic materials. Extensive experimental data are now available on the principal magnetic properties (magnetic ordering temperature, saturation magnetization, magnetic structure, etc.) of the compounds of uranium with various elements. However, many important and interesting features of the magnetism of these compounds—such as the nature of the magnetic order, degree of localization of the magnetic moment of the uranium ions, influence of the crystal field on this moment, etc.—are known only partially. This is largely due to the fact that the published investigations of the magnetic properties of uranium compounds have not been sufficiently comprehen-

sive and have been carried out primarily on polycrystalline samples, so that there is little information on such important characteristics as the magnetic anisotropy and magnetostriction.

The compound UGa_2 is attracting considerable attention. It is the only compound of uranium with the hexagonal $A1B_2$ -type structure and ferromagnetic ordering at low temperatures. Measurements of the magnetization, magnetostriction, paramagnetic susceptibility, electrical resistivity, and Young modulus have been carried out¹⁻¹⁰ on polycrystalline samples of UGa_2 . However, the magnetic properties obtained for polycrystalline samples can only be regarded as estimates because of the exceptionally strong magnetic anisotropy of this compound (see below). In view of this situation, it seemed desirable to carry out a systematic investi-

gation of the magnetic properties, magnetostriction, and crystal structure of UGa_2 single crystals throughout the complete range of temperatures of the magnetically ordered state.

2. SAMPLES AND EXPERIMENTAL METHOD

The compound UGa_2 was synthesized by fusing together the components in a water-cooled copper tray in a helium-filled arc furnace. The grain size was increased by heating the resultant ingot to the melting point (1200°C) in an Alundum crucible placed inside a resistance furnace. The chemical activity of uranium resulted in the formation of a uranium oxide film on the surface so that an ingot actually melted in an oxide "crucible." This prevented the interaction between the uranium and the Alundum crucible. A high ($\sim 150^\circ\text{C}/\text{cm}$) temperature gradient during cooling made it possible to prepare UGa_2 ingots with fairly large grains from which single crystals of mass up to 300 mg were cut. The x-ray diffraction data indicated that these crystals did not contain more than 5% of the UGa_3 phase. The misorientation of the subgrain boundaries did not exceed 2° .

The crystal lattice parameters were determined by the x-ray method using a Gegerfleks diffractometer in the temperature range $4.2\text{--}300^\circ\text{K}$; this was done for single crystals and powders. In the latter case, use was made of a powder prepared by grinding an ingot in a mortar or a powder prepared by diffusion sintering of uranium and gallium in the appropriate proportions at 250°C , followed by annealing at 600°C (Ref. 5). This powder contained approximately the same amount of the UGa_3 phase but was finer than the powder prepared by grinding an ingot and, moreover, in contrast to the latter, it did not have metallic luster.

The magnetization and susceptibility were measured on single crystals along various crystallographic directions using an induction method and static fields up to 75 kOe at 4.2°K and up to 38 kOe in the temperature range $4.2\text{--}300^\circ\text{K}$. The paramagnetic susceptibility was measured with a vibration magnetometer and pendulum balance in fields up to 10 kOe at $130\text{--}300^\circ\text{K}$. The magnetostriction was determined in pulsed magnetic fields (pulse duration ~ 5 nsec) in the temperature range $4.2\text{--}130^\circ\text{K}$ using a portable piezoelectric transducer.¹¹

3. CRYSTAL STRUCTURE

The crystal structure of UGa_2 at $T=300^\circ\text{K}$, i.e., in the paramagnetic state, is hexagonal and of the $A1B_2$ -type with the space group $P6/mmm$ and lattice parameters $a=4.2130$ Å, $c=4.0171$ Å in the case of the powder prepared from an ingot, and $a=4.2103$ Å, $c=4.0193$ Å in the case of the powder synthesized by diffusion sintering (Fig. 1a). The following values of these parameters are reported in the literature: $a=4.21$ Å, $c=4.01$ Å (Ref. 1); $a=4.212$ Å, $c=4.024$ Å (Ref. 2); $a=4.22$ Å, $c=4.02$ Å (Ref. 3). The small differences between the lattice parameters measured on different samples by different authors may be due to the existence of a homogeneity region of the compound UGa_2 or to the influence of mechanical stresses.

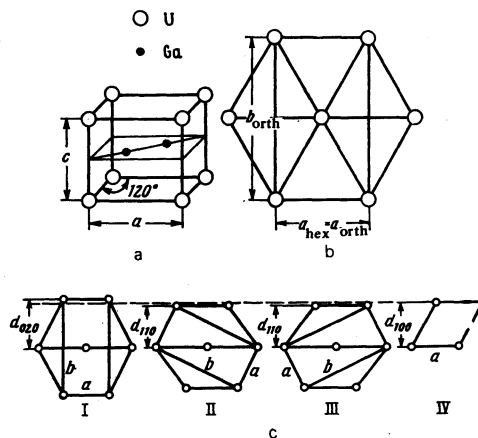


FIG. 1. a) Hexagonal unit cell of UGa_2 . b) Relationship between the hexagonal and orthorhombic cells in the (001) plane. c) Appearance of two distances between the (100) hexagonal planes as a result of magnetic ordering: I-III are magnetic phases with different directions of the easy axis; IV is the undistorted hexagonal cell.

The temperature dependences of the lattice parameters of UGa_2 are plotted in Fig. 2. Cooling results in a linear reduction in the parameters in the paramagnetic temperature range and there are no anomalies in the dependences $a(T)$ and $c(T)$ in the range $130\text{--}300^\circ\text{K}$. Hence, it follows that there are no structural transitions in this range such as those suggested in Ref. 4 to explain the experimentally detected thermal hysteresis of the electrical resistivity and Young modulus at such temperatures.

Cooling below the magnetic ordering temperature splits all the diffractogram lines, with the exception of (00l). This shows that the hexagonal structure becomes distorted (Fig. 1b) and is converted to the orthorhombic space group $Cmmm$. The distortions can be defined as $\Delta = b/\sqrt{3} - a$ and it is clear from Fig. 2 that the value of Δ increases monotonically on reduction in temperature of the sample prepared from the ingot.²⁾

The orthorhombic distortions of the crystal structure of UGa_2 associated with the magnetostrictive strains, which appear in the magnetically ordered state, are evidence of a strong magnetostriction. The relationship between the crystal lattice distortions and magnetostriction will be discussed in greater detail later. Here, we note that, according to x-ray measurements on a single crystal, the (h00) reflections (with hexagonal indices) split into two lines: (02h0) and (hh0)

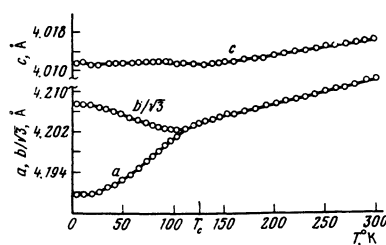


FIG. 2. Temperature dependences of the crystal lattice parameters of UGa_2 .

(orthorhombic indices) in the magnetically ordered state. This corresponds to two different interplanar distances in a crystal perpendicular to the same direction. This is due to the fact that, in the magnetically ordered state, a crystal splits into different magnetic phases (domains) in which the magnetization directions and, consequently, the magnetostrictive strains are oriented along the various easy magnetization directions (a axes) in the basal plane. Since the number of such easy axes and, consequently, possible magnetic phases is three-transition to the magnetically ordered state splits a crystal into trillings of different magnetic phases so that the sample as a whole ceases to be a single crystal: each of the split regions is then a single crystal. In the demagnetized state with the equilibrium domain structure, i.e., when the volumes of the different magnetic phases are equal, the $(hh0)$ line should be twice as strong as the $(02h0)$ line (Fig. 1c), which is indeed observed experimentally.

4. MAGNETIC MOMENT AND MAGNETIC ANISOTROPY

Figure 3 shows the magnetization curves of a UGa_2 single crystal along various crystallographic directions at $4.2^\circ K$. We can see that the hexagonal c axis of the [001] crystal is a difficult-magnetization direction and the directions of easy magnetization lie in the basal plane along the a axes (type $\langle 100 \rangle$ directions).

Figure 4 shows the temperature dependence of the spontaneous magnetization σ_s of UGa_2 , found from magnetic measurements along the easy axis. The dependence $\sigma_s(T)$ obtained for UGa_2 is typical of ferromagnets. The Curie temperature, deduced from the Landau theory of second-order phase transitions using the dependences $\sigma^2 = f(H/\sigma)$ is $125^\circ K$, which is close to the results reported in Ref. 5 and 6.

The magnetic moment μ_V per uranium atom in UGa_2 is $2.71 \mu_B$ at $4.2^\circ K$. This value is greater than μ_V found in Refs. 6 and 7 from magnetic measurements on polycrystalline samples (up to $2.35 \mu_B$), which is due to the fact that in both investigations the samples were not saturated in the magnetic fields employed. It is also considerably greater than $\mu_V = 2.28 \mu_B$, found from neutron-diffraction data.⁵ This difference may be due to the fact that the value of μ_V was calculated in Ref. 5 using the neutron-scattering form factor obtained on the assumption that the magnetic moment of the uranium ions in UGa_2 was of purely spin origin. Clearly, this

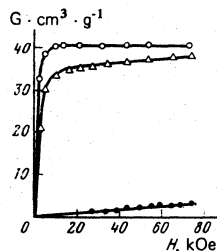


FIG. 3. Magnetization curves of a UGa_2 single crystal along various axes at $4.2^\circ K$: \circ) [100] (a axis); Δ) [120] (b axis); \bullet) [001] (c axis) (hexagonal indices).

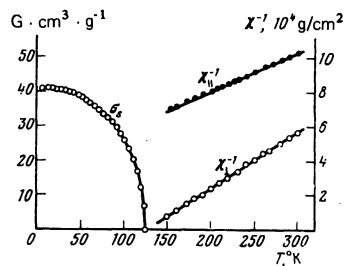


FIG. 4. Temperature dependences of the specific spontaneous magnetization σ_s and reciprocal susceptibility χ^{-1} : \circ) measurements along the [100] axis; \bullet) measurements along the [001] axis.

assumption is incorrect. The difference between the values of the magnetic moments of uranium in UGa_2 , deduced from the magnetic and neutron-diffraction measurements, may be due to reasons other than the methodological factor just mentioned. A similar difference in the case of some actinide compounds is explained by the presence of a delocalized spin density associated with the conduction-electron polarization.¹² This may also apply to UGa_2 .

Figure 4 shows the dependences of the reciprocal paramagnetic susceptibilities χ_1^{-1} and χ_2^{-1} , obtained in magnetic fields oriented along the c and a axes, respectively. (It follows from our measurements that the susceptibility anisotropy in the basal ab plane is slight.) In both cases, the susceptibility obeys the Curie-Weiss law. In the basal plane, the paramagnetic Curie temperature is $\Theta_p^+ = 127^\circ K$ and the effective magnetic moment is $\mu_{\text{eff}}^+ = 3.0 \mu_B$. The susceptibility along the c axis is considerably less and the paramagnetic Curie temperature along this direction is negative: $\Theta_p^- = -148^\circ K$; the effective magnetic moment is $\mu_{\text{eff}}^- = 3.55 \mu_B$. The considerable anisotropy of the paramagnetic susceptibility has already been reported for the ferromagnetic compounds UAs and $UAsSe$ (Ref. 13) with the tetragonal crystal structure and it has been found, exactly as in the case of UGa_2 , that Θ_p along the easy magnetization direction is close to the magnetic ordering temperature, whereas in the difficult magnetization direction the value of Θ_p is negative. However, in the case of UAs and $UAsSe$, the effective magnetic moment is independent of the direction.³⁾

The differences between the values of μ_{eff} indicate that the Curie-Weiss law cannot be used to describe the temperature dependence of the magnetic susceptibility of UGa_2 in the form $\chi = c/(T - \Theta_p)$. Therefore, we shall assume that this difference is due to the fact that the susceptibility of UGa_2 includes, in addition to the contribution obeying the Curie-Weiss law, a temperature-independent component χ_0 due to the delocalized component of the magnetic moment. An analysis of the experimental data carried out allowing for the temperature-independent contribution shows that the susceptibility of UGa_2 in the basal plane and along the c axis can be described by

$$\chi(T) = \chi_0 + c/(T - \Theta_p), \quad (1)$$

where $\chi_0 = 2.8 \times 10^{-6}$ and $c = 2.57 \times 10^{-3} \text{ }^\circ K$, which cor-

responds to $\mu_{\text{eff}} = 2.8 \mu_B$. We then find that $\Theta_p = -64^\circ \text{K}$ and $\Theta_p^1 = 134^\circ \text{K}$.

It follows from Fig. 3 that the compound UGa_2 is characterized by a strong magnetic anisotropy: at 4.2°K in a field of 75 kOe, the saturation cannot be attained not only along the hexagonal axis, which is the direction of the most difficult magnetization, but also in the basal plane along the b ($\langle 120 \rangle$) axis. The magnetic anisotropy energy of a hexagonal crystal can be written in the form

$$E_a = K_1 \sin^2 \theta + K_2 \sin^4 \theta + K_3 \sin^6 \theta \cos 6\varphi, \quad (2)$$

where θ is the angle between the magnetization and the c axis, and φ is the angle between the magnetization and b axis in the basal plane. The first two terms in Eq. (2) describe the uniaxial anisotropy and the third represents the hexagonal anisotropy in the basal plane of the crystal.

In weak fields, the magnetization along the c axis is proportional to the field:

$$\sigma = -H\sigma_s^2 / 2(K_1 + 2K_2). \quad (3)$$

We can use the above formula to determine the uniaxial magnetic anisotropy of UGa_2 . It is found that $K_1 + 2K_2 = -2 \times 10^7 \text{ erg/g}$ at 4.2°K , which corresponds to the anisotropy field $H_A = 2(K_1 + 2K_2) / \sigma_s \approx 10^6 \text{ Oe}$. This represents the lower limit of the uniaxial magnetic anisotropy of UGa_2 because the misorientation of subgrains and the field orientation (the combined effect may be up to 2°) increase the magnetization along the hexagonal axis and thus reduce the anisotropy. Allowance for these errors show that the anisotropy field is within the range $(1-15) \times 10^6 \text{ Oe}$.⁴⁾

The uniaxial magnetic anisotropy in the magnetically ordered state and the anisotropy of the paramagnetic susceptibility are related. If the effective magnetic moments of the uranium ions are the same along different crystallographic directions and if the anisotropy energy depends on temperature as $\sigma_s^2(T)$, the application of the Landau theory of phase transitions gives¹⁴⁾

$$H_A = (\chi_{\parallel}^{-1} - \chi_{\perp}^{-1}) \sigma_s. \quad (4)$$

This formula and the paramagnetic susceptibility of UGa_2 gives $H_A = 3 \times 10^6 \text{ Oe}$ at 4.2°K , which is in order-of-magnitude agreement with the estimate of H_A deduced from the magnetic measurements at the same temperature.⁵⁾

The uniaxial anisotropy of UGa_2 is strong at all temperatures below the Curie point. This is clear from Fig. 5: the field of 32 kOe does not saturate the sample along the c axis not only at low temperatures but also near the Curie point. It also follows from Figs. 3 and 5 that the anisotropy in the basal plane is strong. However, a field of 32 kOe applied above 90°K does saturate the sample in the $\langle 120 \rangle$ direction.

A simple calculation shows that, in relatively weak fields oriented in the basal plane along the b axis, the magnetization varies linearly with the field:

$$\sigma = 1/2 \sigma_s \sqrt{3} + \sigma_s^2 H / 72 K_s. \quad (5)$$

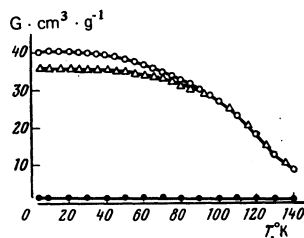


FIG. 5. Temperature dependences of the specific magnetization in a field of 32 kOe along different crystallographic directions: ○ [100]; △ [120]; ● [001].

Hence, the experimental data (Fig. 3) give $K_3 = -0.6 \times 10^6 \text{ erg/g}$ at $T = 4.2^\circ \text{K}$.

5. COERCIVE FORCE

Single crystals of UAsSe have a high coercive force ($H_c \sim 10 \text{ kOe}$) at $T = 4.2^\circ \text{K}$ when magnetized along the easy axis.¹⁵ This high value of H_c of bulk single crystals seems to be due to delay in the displacement of domain walls which are narrow because the magnetic anisotropy is very strong and its energy is comparable with the exchange energy. The wall width δ amounts to a few lattice parameters. Therefore, the coercivity of the walls is high:¹⁶⁾

$$H_w = \pi H_A \Delta\gamma / 4Kd = \pi \Delta\gamma / 2dI_s, \quad (6)$$

where $\Delta\gamma$ is the maximum change in the domain wall energy in the course of its displacement in a perfect crystal and d is the wavelength of the Peierls potential.

In view of this, it seemed interesting to determine the value of H_c of our UGa_2 compound, which has a uniaxial magnetic anisotropy of the same order of magnitude but a weaker anisotropy in the ab basal plane. Figure 6 shows a hysteresis loop of a UGa_2 single crystal magnetized along the a axis at 4.2°K and the temperature dependence of the coercive force. We can see that H_c at 4.2°K is 1.1 kOe, which is much less than for UAsSe . This is due to the fact that the domain walls in the easy-plane UGa_2 are of the Néel type, in contrast to the magnetically uniaxial UAsSe , where they are of the Bloch type. In the former case, the magnetization vector does not rotate in the ac plane, as in UAsSe , but in the ab plane and mainly against the forces of the relatively weak anisotropy in the basal plane ($K_3 = -0.6 \times 10^6 \text{ erg/g}$). Estimates indicate that the wall width is 10^2 \AA , which is approximately an or-

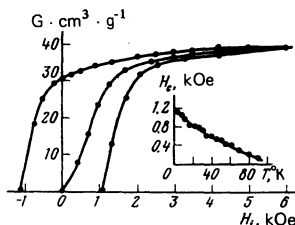


FIG. 6. Magnetization curve and hysteresis loop of a single crystal at 4.2°K in an internal field H_i (measurements along the [100] axis). The inset shows the temperature dependence of the coercive force.

der of magnitude higher than that for UAsSe. Therefore, in our case, the wall coercivity H_w should be considerably less because of the exponential dependence of H_w on δ :

$$H_w \propto e^{-\pi\delta/d} \quad (7)$$

The coercive force in UGa_2 is due to the domain-wall coercivity and clearly also due to the fact that the wall displacement is hindered by lattice defects in single crystals and, possibly, due to changes in the magnetoelastic energy as a result of wall displacement.

6. MAGNETOSTRICTION

The magnetostriction of a hexagonal crystal can be represented in the form¹⁷

$$\lambda = \lambda_1^{\alpha_1^2} (\beta_1^2 + \beta_2^2) + \lambda_2^{\alpha_2^2} \beta_2^2 + \lambda_3^{\alpha_1^2} (\beta_1^2 + \beta_2^2) (\alpha_1^2 - 1/3) + \lambda_4^{\alpha_2^2} \beta_2^2 (\alpha_2^2 - 1/3) + \lambda_5^{\alpha_1^2} [1/2 (\beta_1^2 - \beta_2^2) (\alpha_1^2 - \alpha_2^2) + 2\beta_1\beta_2\alpha_1\alpha_2] + 2\lambda_6^{\alpha_1^2} (\beta_1\alpha_1 + \beta_2\alpha_2) \beta_3\alpha_3 \quad (8)$$

Here, α_i are the direction cosines of the magnetization and β_i are the direction cosines of the direction of strain measurement. The first two terms describe the paraprocession magnetostriction depending solely on the direction of measurement and the other terms describe the magnetostriction which also depends on the orientation of the magnetization relative to the crystallographic axes.

This formula readily shows that the longitudinal magnetostriction in the basal plane along an easy magnetization axis a is

$$\lambda_a^{\parallel} = \lambda_1^{\alpha_1^2} / 2, \quad (9)$$

and the longitudinal magnetostriction in the basal plane along the b axis in weak fields (in this case, we can ignore deviations of the magnetic moments from the a axes nearest to the b axis) is

$$\lambda_b^{\parallel} = \lambda_1^{\alpha_1^2} / 4. \quad (10)$$

Figure 7 shows the field dependences of the longitudinal magnetostriction of a UGa_2 single crystal in the basal plane along the a and b axes. We can see that the condition $\lambda_a^{\parallel} = 2\lambda_b^{\parallel}$, which follows from Eqs. (9) and (10), is now satisfied. [Some departure from this condition is clearly due to the fact that the domain structures of the investigated samples differ from equilibrium, assumed in the derivation of Eqs. (9) and (10).]

The temperature dependences of $\lambda^{\gamma,2}$, deduced from Eqs. (9) and (10), are plotted in Fig. 8. We can see that the magnetostriction of UGa_2 is very high: at 4.2° K,

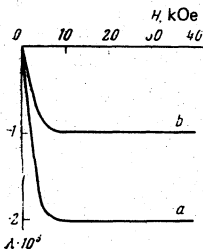


FIG. 7. Field dependence of the longitudinal magnetostriction of a UGa_2 single crystal at 4.2°K along the [100] (a) and [120] (b) axes.

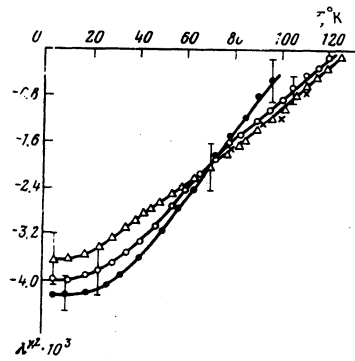


FIG. 8. Temperature dependences of the magnetostriction $\lambda^{\gamma,2}$ obtained from magnetostriction measurements along various axes: \circ) [100]; Δ) [120]; \times) polycrystalline sample; \bullet) deduced from lattice parameters.

the value of $\lambda^{\gamma,2}$ reaches $\sim 4 \times 10^{-3}$, which is comparable with the magnetostriction of rare earths.¹⁸

The magnetostriction of a polycrystalline sample of UGa_2 was measured above 78°K in Ref. 4. Averaging over the weak-field magnetostriction of a polycrystalline sample, when we can assume that the magnetization does not deviate from the type a axes nearest to the field, gives

$$\lambda^{\gamma,2} = \lambda_1^{\alpha_1^2} / 4. \quad (11)$$

The values of $\lambda^{\gamma,2}$ calculated using the above formula and the data on the magnetostriction of a polycrystalline sample⁴ are in good agreement with the data obtained for single crystals (Fig. 8).

It is interesting to estimate also the magnetostriction of UGa_2 from the temperature dependences of the lattice parameters (Fig. 2). If, as is true of UGa_2 , the magnetization lies in the basal plane along type a axes, Eq. (8) yields the following expressions for the lattice parameters in the ferro-magnetic state:

$$\begin{aligned} a/a_{\text{para}} - 1 &= (\lambda_1^{\alpha_1^2} - 1/3\lambda_3^{\alpha_1^2}) + 1/2\lambda_1^{\alpha_1^2}, \\ b/b_{\text{para}} - 1 &= (\lambda_1^{\alpha_1^2} - 1/3\lambda_3^{\alpha_1^2}) - 1/2\lambda_1^{\alpha_1^2}, \quad c/c_{\text{para}} - 1 = \lambda_2^{\alpha_2^2}, \end{aligned} \quad (12)$$

where a_{para} , b_{para} , and c_{para} are the lattice parameters without allowance for magnetoelastic interaction. Since $b_{\text{para}} = a_{\text{para}}\sqrt{3}$, it follows from the formulas of Eq. (12) that

$$\lambda^{\gamma,2} = (a - b/\sqrt{3})/a_{\text{para}}. \quad (13)$$

The values of $\lambda^{\gamma,2}$, calculated from the x-ray data, are plotted in Fig. 8. We can see that, within the limits of the experimental error, they agree with the values of the same constant deduced from the magnetostriction measurements in a magnetic field.

The temperature dependences of the lattice parameters also allow us to estimate other magnetostriction constants. It follows from Eq. (12) that

$$\lambda_1^{\alpha_1^2} - 1/3\lambda_3^{\alpha_1^2} = [(a + b/\sqrt{3}) - 2a_{\text{para}}]/2a_{\text{para}}, \quad \lambda_2^{\alpha_2^2} = (c - c_{\text{para}})/c_{\text{para}}. \quad (14)$$

However, in the calculation of these constants, we have to know the lattice parameters without allowance for magnetoelastic interaction at a given temperature:

a_{para} , b_{para} , and c_{para} . They can be calculated using the Grüneisen relationship for the temperature dependence of the thermal expansion coefficient¹⁹

$$\alpha = A c_V \quad (15)$$

(c_V is the specific heat at constant volume and the coefficient A is independent of temperature) together with the experimental temperature dependences of the lattice parameters of UGa_2 in the paramagnetic region. In these calculations, we have to know the temperature dependence of c_V , i.e., the value of the Debye temperature Θ_D , which can be estimated—because of the absence of experimental data—from the Lindemann formula¹⁹

$$\Theta_D = 137 (T_{\text{mp}}/V^{1/3}M)^{1/2} \approx 100^\circ\text{K}, \quad (16)$$

where T_{mp} is the melting point, M is the molecular weight, and V is the molecular volume of UGa_2 . Then, at 4.2°K , we have $\lambda_2^{\alpha,0} = 0.9 \times 10^{-3}$, and the value of $\lambda_1^{\alpha,0} - \frac{1}{3}\lambda_1^{\alpha,2}$ is close to zero. We note that these values are estimates and can be refined when the experimental value of the Debye temperature of UGa_2 becomes available.

7. CONCLUSIONS

It is generally assumed that the $5f$ electrons in metallic uranium are in the collective state.²⁰ In compounds of uranium with other elements, the distance between the uranium ions is greater than in the pure metal and this gives rise to a state with localized $5f$ electrons, such as that observed in—for example— UX ($X = \text{As}, \text{P}, \text{S}$) compounds,^{21,22} although even in these compounds the overlap of the wave functions of the $5f$ electrons and the $6d$ and $7s$ conduction electrons is considerable.²² In the group of compounds with stoichiometric composition close to UX_2 , which includes UGa_2 and the compounds UB_2 , UHg_2 , and U_3Si_5 with the same crystal structure, the U-U distances are close to the critical value at which there is a transition of the $5f$ electrons from the collective to the localized state.³ Therefore, the properties of such compounds depend strongly on the interatomic distances (UGa_2 is a ferromagnet, UB_2 is a paramagnet with a temperature-independent susceptibility, U_3Si_5 is a paramagnet whose susceptibility obeys the Curie-Weiss law, and UHg_2 is an antiferromagnet³).

The magnetic moment of uranium ions in UGa_2 , found by us to be $\mu_U = 2.71 \mu_B$, does not agree with the magnetic moments of uranium ions of different valences calculated by the Russell-Saunders scheme: $\mu_U = gJ\mu_B$ ($\mu_U = 3.28 \mu_B$ for U^{3+} , $\mu_U = 3.20 \mu_B$ for U^{4+} , and $\mu_U = 2.14 \mu_B$ for U^{5+}). It follows that the uranium ions are not free in the ferromagnetic state of UGa_2 . The difference between μ_U and the value of gJ is probably due to partial delocalization of the $5f$ electrons and the influence of the crystal field on the energy spectrum of uranium ions.

Unfortunately, quantitative estimates of the crystal field in UGa_2 are lacking but we can use the results for other uranium compounds (see, for example, Refs. 23 and 24) to conclude that the high magnetocrystalline

anisotropy energy of UGa_2 is mainly due to the interaction of the anisotropic cloud of the $5f$ electrons with the ligand crystal field, and is of single-ion nature. The giant magnetostriction of this compound is, in its turn, related to the strong dependence of the crystal field parameters on the interatomic distances.

The authors are grateful to B. V. Mill', Z. Smetana, and V. Sechovský for valuable discussions.

¹Charles University, Prague, Czechoslovakia.

²Distortions of the crystal structure of a sample prepared by diffusion sintering are, at 4.2°K , of about the same magnitude but depend nonmonotonically on temperature: at 37°K , the value of $\Delta(T)$ passes through a minimum. The reasons for this discrepancy are not clear. It may be due to different compositions of the samples prepared by different methods. Since the samples prepared by diffusion sintering are powders, their magnitude and magnetostriction properties cannot be investigated properly. Therefore, we shall only discuss the magnetization and magnetostriction measurements carried out on single crystals cut from an ingot.

³Measurements of the paramagnetic susceptibility of UGa_2 were carried out on several single crystals by various methods. An analysis also shows that the difference between the values of $\mu_{\text{eff}}^{\parallel}$ and μ_{eff}^{\perp} cannot be explained by errors in the orientation of the samples during measurements.

⁴It should be noted that the uniaxial magnetic anisotropy energy of UGa_2 is comparable with the exchange interaction energy because an estimate deduced from the Curie temperature gives the exchange field $H_E = kT_C/\mu_1 \approx 0.7 \times 10^6$ Oe; therefore, it is not quite correct to describe the magnetic anisotropy by Eq. (2) obtained on the assumption that the anisotropy energy can be regarded as a small perturbation compared with the exchange energy.

⁵The temperature-independent contribution to the susceptibility is allowed for in the calculations.

¹E. S. Makarov and V. A. Levdiĭk, *Kristallografiya* 1, 644 (1956) [*Sov. Phys. Crystallogr.* 1, 506 (1956)].

²K. H. J. Buschow, *J. Less-Common Met.* 31, 165 (1973).

³A. Misiuk, J. Mulak, A. Czopnik, and W. Trzebiatowski, *Bull. Acad. Pol. Sci. Ser. Sci. Chim.* 20, 337 (1972).

⁴R. Z. Levitin, A. S. Dmitrievskii, Z. Henkie, and A. Misiuk, *Phys. Status Solidi A* 27, K109 (1975).

⁵V. Sechovský, Z. Smetana, and A. Meňovský, *Phys. Status Solidi A* 28, K37 (1975).

⁶J. Šternberk, J. Hřebík, A. Meňovský, and Z. Smetana, *J. Phys. (Paris)* 32, Colloq. 1, C1-744 (1971).

⁷K. H. J. Buschow and H. J. van Daal, *AIP Conf. Proc. No.* 5, 1464 (1971).

⁸V. Ansgorge and A. Meňovský, *Phys. Status Solidi* 30, K31 (1968).

⁹K. P. Belov, Z. Henkie, A. S. Dmitrievskii, A. Zygmunt, R. Z. Levitin, and Yu. F. Popov, *Proc. Intern. Conf. on Magnetism, Moscow, 1973, Vol. 6, Nauka, M., 1974, p. 54.*

¹⁰Z. Smetana, V. Houdek, A. Meňovský, and Z. Šimsá, *Phys. Status Solidi A* 28, K103 (1975).

¹¹B. K. Ponomarev and R. Z. Levitin, *Prib. Tekh. Eksp. No. 3*, 188 (1966).

¹²A. T. Aldred, B. D. Dunlap, and G. H. Lander, *Phys. Rev. B* 14, 1276 (1976).

¹³K. P. Belov, A. S. Dmitrievskii, A. Zygmunt, R. Z. Levitin, and W. Trzebiatowski, *Zh. Eksp. Teor. Fiz.* 64, 582 (1973) [*Sov. Phys. JETP* 37, 297 (1973)].

- ¹⁴A. S. Dmitrievskii, Avtoreferat kand. diss. (Author's Abstract of Thesis for Candidate's Degree), Moscow State University, 1973.
- ¹⁵C. Bazan and A. Zygmunt, Phys. Status Solidi A 12, 649 (1972).
- ¹⁶H. R. Hiltzinger and H. Kronmüller, Phys. Status Solidi B 54, 593 (1972).
- ¹⁷E. Callen and H. B. Callen, Phys. Rev. 139, A455 (1965); A. Clark, R. Bozorth, and B. de Savage, Phys. Lett. 5, 100 (1963).
- ¹⁸K. P. Belov, M. A. Belyanchikova, R. Z. Levitin, and S. A. Nikitin, Redkozemel'nye ferro- i antiferromagnetiki (Rare-Earth Ferromagnets and Antiferromagnets), Nauka, M., 1965.
- ¹⁹S. I. Novikova, Teplovoe rasshirenie tverdykh tel (Thermal Expansion of Solids), Nauka, M., 1974.
- ²⁰J. Friedel, J. Phys. Radium 19, 573 (1958).
- ²¹F. A. Wedgwood and M. Kuznietz, J. Phys. C. 5, 3012 (1972).
- ²²J. M. Robinson and P. Erdős, Phys. Rev. B 8, 4333 (1973); 9, 2187 (1974).
- ²³R. Troč, J. Mulak, and W. Suski, Phys. Status Solidi B 43, 147 (1971).
- ²⁴J. Przystawa and E. Praveczi, J. Phys. Chem. Solids 33, 1943 (1972).

Translated by A. Tybulewicz

The Mott transition in the many-dimensional Hubbard model

R. O. Zaitsev

Kurchatov Atomic Energy Institute

(Submitted 17 July 1978)

Zh. Eksp. Teor. Fiz. 75, 2362-2374 (December 1978)

The phase transition problem is solved in the approximation of a large number of nearest neighbors. A phenomenological theory is constructed to find the density of states and the value of the dielectric gap in the neighborhood of the critical point. Concrete calculations are made for the BCC and simple cubic lattices. A detailed comparison with the results of Hubbard's work [Proc. Roy. Soc. A281, 401 (1964)] shows qualitative but not quantitative agreement. The problem of finding the density of states in a metallic phase far from the transition point is discussed.

PACS numbers: 72.60. + g, 71.20. + c

INTRODUCTION

We shall study the Hubbard model under the conditions that the number of electrons is equal to the number of sites and the density of states is an even function of the energy. Simple examples that will be considered are the d -dimensional BCC and simple cubic lattices, and also a hypothetical model with the density of states given by Eq. (7), which is the same in zeroth approximation as that used by Hubbard.¹ In all of these cases at $T=0$ the ground state is nearly antiferroelectric, for any value of the ratio of the energy t for transition of an electron to an adjacent cell to the intraatomic exchange energy I . In papers by Langer, Plischke, and Mattis² and by the present writer³ it has been shown by extrapolation that at the Mott transition point the value of the Neél temperature T_N is at least an order of magnitude smaller than the exchange energy I . Using this as an assumption, we shall consider the metal-dielectric transition (M transition) in a paraphase, regarding the temperature as small compared with I but large compared with T_N .

For this temperature range an attempt has been made

to construct a phenomenological theory of the M transition appropriately analogous to the theory of gapless superconductivity.⁴ A rigorous calculation can be made only in a space of a large number of dimensions. It will be shown that this scheme checks qualitatively with almost all of the results of the Hubbard theory¹ that are correct above the Neel temperature. It turns out that for the density of states (7) the critical value of the ratio t/I is identical with the value found in Ref. 1, but otherwise the results are quantitatively different.

1. THE APPROXIMATION OF LARGE NUMBER OF NEAREST NEIGHBORS

In a nonmagnetic phase, when $T_N \ll T \ll I$, we can take the Hubbard solution¹ as a zeroth approximation. The corresponding G function will be written in the notation of the previous papers by the writer^{3,5}:

$$G_{\sigma,\sigma}^{-1}(\mathbf{k}) = \begin{pmatrix} (0, \sigma) & (0, \sigma) & (-\sigma, 2) \\ (0, \sigma) & (-i\omega_n - \varepsilon_0 - 1/2 t(\mathbf{k}), & -1/2 \sigma t(\mathbf{k}) \\ (-\sigma, 2) & -1/2 \sigma t(\mathbf{k}), & -i\omega_n + \varepsilon_0 - 1/2 t(\mathbf{k}) \end{pmatrix}, \quad (1)$$

$$t(\mathbf{k}) = t \sum_{\langle \mathbf{r} \rangle} e^{i\mathbf{k}\cdot\mathbf{r}}, \quad \varepsilon_0 = 1/2 I, \quad \omega_n = (2n+1)\pi T.$$